GAS PATH DIAGNOSIS METHOD FOR GAS TURBINE FUSING PERFORMANCE ANALYSIS MODELS AND EXTREME LEARNING MACHINE

by

Shiyao LI[a*], Zhenlin LI[b], Meng ZHANG[a], and Song HAN[a]

[a] PipeChina Beijing Pipe-line Co., Ltd., Beijing, China
[b] College of Mechanical and Transportation Engineering,
China University of Petroleum (Beijing), Beijing, China

Original scientific paper
https://doi.org/10.2298/TSCI220509018L

The gas path analysis, which can quantify the performance degradation of gas turbine components, has been extensively applied to the gas path diagnosis. However, the precondition of this method is that the number of measurable parameters for the gas turbine to be diagnosed should not be less than the number of its health factors. In the existing research, this precondition can be guaranteed through common approaches such as screening the degraded components by a model-based prediagnosis process or recognizing the degraded components by using tools such as an ANN or a support vector machine. However, the diagnosis speed, recognition accuracy, and robustness of these approaches need to be improved. Therefore, a diagnosis method fusing the gas path performance analysis model and the extreme learning machine was proposed in this paper and applied to a GE LM2500+SAC gas turbine. The working mechanism of similarity ranking-gas path diagnosis-rationality check was introduced in the fusion method, endowing it with a higher recognition accuracy rate, stronger robustness, and higher diagnostic accuracy.

Key words*: gas turbine, performance degradation, gas path diagnosis, extreme learning machine, pattern recognition, smearing effect*

Introduction

Gas turbines have been widely used in numerous fields such as aviation, ship, and electric power because of their high efficiency, high unit power, and long service life. Especially when applied to natural gas pipe-lines, gas turbine-driven compressor sets, which can considerably reduce the local power grid load, are the preferred equipment in areas with underdeveloped electric power supply.

The main gas path components of a gas turbine work under environments with high temperatures, high pressures, high rotation speeds, and large flow quantities. Fouling, corrosion, wear, and ablation, among other factors, will unavoidably appear on the compressor blade or the turbine blade as a result of the unfiltered dust in the atmosphere, the corrosive components in the combustion products, the friction between the blades and cavity, and the carbon deposition formed on the nozzle of the combustion chamber (CC) [1]. These problems will result in degrading thermal efficiency and declining output power of the gas turbine [1, 2], or,

* Corresponding author, e-mail: lishiyao@126.com

even worse, lead to unexpected halts and component damage. Therefore, the key to the safe, steady, and efficient operation of gas turbines lies in the timely and accurate mastering of the health conditions of each component. This is also of great importance for formulating a reasonable maintenance and repair plan and the advance purchase of spare parts [3].

Since being proposed by Urban [4] in 1973, gas path analysis (GPA) – a gas turbine diagnosis method based on the thermodynamic model – has been fully developed and extensively applied [3]. For both the linear and non-linear diagnosis methods [4-7], a necessary condition for obtaining unique solutions of diagnosis equations is that the number of gas path measurable parameters should be greater than or equal to that of the components' health factors. Otherwise, nearly all components will be diagnosed with gas path performance degradation, referred to as the smearing effect [3, 8].

The methods to avoid the smearing effect can be roughly divided into two categories. The first category addresses gas path diagnosis based on a thermodynamic model: by increasing the number of governing equations based on prior information, or by reducing the number of undetermined health factors through a screening process, the diagnosis equations will have a unique solution. The second category recognizes the components within the performance degradation by using a pattern recognition tool. Therefore, a qualitative diagnosis can be realized without solving the diagnosis equations.

Previous researchers have widely explored these two categories. Stamatis *et al.* [9] put forward the discrete operating conditions gas path analysis (DOCGPA), expanding the dimension of diagnosis equations using gas path measurable parameters under multiple operating points to acquire unique solutions. Mathioudakis *et al.* [10] proposed a non-linear-model-based method for tracking components' performance degradation: while determining the deviation direction of components' health factors, their diagnosed values at previous instance were determined as the best guesses of the present moment because the performance degradation of components was a slow process. Aretakis *et al.* [11] and Macthioudakis *et al.* [12] introduced a model-based prediagnosis process before performing the quantitative diagnosis. This process aimed to screen for the components that were significantly degraded. In both papers, the concept of diagnosis index was introduced, and it quantified the screening basis. However, the real-time feature of these methods was sacrificed as a result of the numerous invocations of the diagnosis model. Borguet *et al.* [13] proposed a constrained least square method for fault isolation. In this method, prior information about the health parameters was derived in the form of constraints. Thus, the isolation capability of the traditional least-squares-based methods could be improved. Nevertheless, this prior information, usually obtained based on the experience of technicians, may not be universal for gas turbines applied to different places with different gas path structures.

In the recent three decades, pattern recognition has been widely applied in various industries. Many approaches primarily represented by the ANN and support vector machine (SVM) have provided an alternative for gas path diagnosis because of their outstanding noise immunity and high computation speed that can be achieved without solving any diagnosis equations.

The back-propagation neural network (BPNN) was applied to gas path diagnosis as early as 1996 [14]. Thereafter, Lu *et al.* [15] introduced the auto-associative neural network to reduce measurement noise, improving the success rate of BPNN-based fault diagnosis. In 2009, Matuck *et al.* [16] studied the fault recognition effect of the multilayer perceptron neural network and achieved a success rate higher than 97%. In the same year, Fast *et al.* [17] explored the quantitative prediction ability of ANN, the results demonstrating that the prediction error of measur-

able parameters could be lower than 1%. Thus, Fast *et al.* [17] indicated that the ANN can be used for gas path performance simulation, condition monitoring, or sensor validation. In 2012, Barad *et al.* [18] adopted a two-hidden-layer ANN to simultaneously monitor the performance and mechanical health of a power turbine (PT). These encouraging results can be obtained in not only a steady-state but transient state.

In terms of SVM-based methods, Zhou *et al.* [19] proposed a stepwise recognition idea in 2015, making it possible to accurately recognize degradation characteristic samples after repeated binary classification. Additionally, the comparison results indicated that SVM can acquire a higher recognition rate when the radial basis function is selected as the kernel function. Huang *et al.* [20] combined the simulated annealing algorithm with GA to optimize the penalty factor and kernel function parameter in SVM, thus improving the recognition rate. Butler *et al.* [21] and Lan *et al.* [22] compared the effects of using different pattern recognition tools, and their results indicated that different tools show their respective recognition preferences. Hence, an effective way to improve the recognition rate lies in fusing the results different pattern recognition tools obtain.

Although they present numerous advantages, pattern recognition-based methods also have defects. For instance, it is difficult to collect gas turbine operating data under typical degradation patterns. Therefore, the data used to train the pattern recognition tools generally derive from simulation models, thus unavoidably leading to a negative impact on the training effect.

In this paper, a gas path diagnosis method fusing the extreme learning machine (ELM) and performance analysis models (simulation model and diagnosis model included) is proposed to eliminate the smearing effect in diagnosis results and guarantee the real-time feature of the diagnosis process. This method has three core steps: first, similarity ranking is conducted between the degradation characteristic samples and all the degradation patterns using ELM. Next, the undetermined health factors under a minority of degradation patterns with high similarity are qualified using the diagnosis model. Finally, only the diagnosis result meeting the criteria of rationality is accepted and output.

Basic theory of ELM

Proposed by Huang [23], ELM is a single-hidden-layer feed-forward neural network. Studies have shown that ELM has a high learning rate and strong generalization ability [24]. Figure 1 shows its typical topological structure.

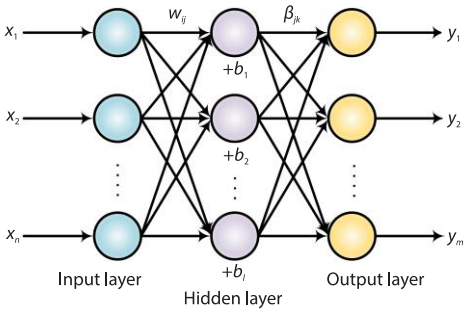

Figure 1. Topological structure of ELM

For a given dataset ($\mathbf{x}_i$, $\mathbf{t}_i$), $i = 1,...,N$, where $\mathbf{x}_i = [x_{i,1}, x_{i,2},...x_{i,n}]^T \in R^n$ and $\mathbf{t}_i = [0, 0,...1,...0]^T \in R^m$ the output of ELM can be defined as:

$$\sum_{i=1}^{l}\boldsymbol{\beta}_i g\left(\mathbf{x}_j\right)=\sum_{i=1}^{l}\boldsymbol{\beta}_i g\left(\mathbf{w}_i\mathbf{x}_j+b_i\right)=\mathbf{t}_j, j=1,2,\cdots N \tag{1}$$

where l is the number of hidden-layer neurons, $\mathbf{w}_i = [w_{i,1}, w_{i,2},... w_{i,n}]^T$, b_i, and $\boldsymbol{\beta}_i = [\beta_{i,1}, \beta_{i,2},...\beta_{i,m}]^T$ are the input weight vector, bias, and output weight vector of the i^{th} hidden-layer neuron, respectively, $\mathbf{w}_i\mathbf{x}_j$ – the inner product of $\mathbf{w}_i$ and $\mathbf{x}_j$, and $g(x)$ – the kernel function. Usually, the sigmoid function, radial basis function, or polynomial function is selected to enhance the non-linear mapping ability of ELM.

Equation (1) can be transformed into a matrix form:

$$\mathbf{H}(\mathbf{w},\mathbf{b})\boldsymbol{\beta} = \mathbf{T} \tag{2}$$

where **H** is the output matrix of the hidden layer, **β** – the output weight matrix of the hidden layer, and **T** – the expected output.

In eq. (2), **H**(**w**, **b**) is uniquely identified because **w** and **b** are randomly determined. Thus, the optimization process of **β** can be further transformed into solving the linear equations:

$$\boldsymbol{\beta} = \mathbf{H}^{\dagger}\mathbf{T} \tag{3}$$

where $\mathbf{H}^{\dagger}$ is the Moore-Penrose generalized inverse of matrix **H**.

As a feed-forward neural network, ELM has a better generalization performance if the norm of **β** is smaller while a smaller training error is reached [25], respectively, the cost function under constrained conditions can be expressed:

$$L = \frac{1}{2}\|\boldsymbol{\beta}\|^2 + C\frac{1}{2}\sum_{i=1}^{N}\|\xi_i\|^2, \text{ s.t.}: \mathbf{h}(\mathbf{x}_i)\boldsymbol{\beta} = \mathbf{t}_i^T - \boldsymbol{\xi}_i^{\mathrm{T}}, \quad i = 1,...N \tag{4}$$

where $\boldsymbol{\xi}_i^T = [\xi_{i,1},... \xi_{i,m}]^T$ represents the error vector of the i^{th} training sample on m output nodes, $\mathbf{h}(\mathbf{x}_i)$ is the output vector of the hidden layer when the sample $\mathbf{x}_i$ is input.

Based on the KKT theorem, the solving process of eq. (4) is equivalent to solving the dual optimization problem and its solving process references [24]:

$$\min(L_{\mathrm{D}}) = \min\left[\frac{1}{2}\|\boldsymbol{\beta}\|^2 + C\frac{1}{2}\sum_{i=1}^{N}\|\boldsymbol{\xi}_i\|^2 - \sum_{i=1}^{N}\sum_{j=1}^{m}\alpha_{i,j}\left(\mathbf{h}(\mathbf{x}_i)\boldsymbol{\beta}_j^* - t_{i,j} + \xi_{i,j}\right)\right] \tag{5}$$

where $\alpha_{i,j}$ is the Lagrange multiplier, $\boldsymbol{\beta}_j^* = [\beta_{1,j}, \beta_{2,j},... \beta_{i,j},]^T$ – the weight vector from the hidden layer to the output node j ($\boldsymbol{\beta}_j^*$ is the transposed matrix of **β**), and C represents a penalty factor.

Equation (6) provides the output equation of the ELM classifier in the case where the number of training samples is much greater than the dimension of feature space:

$$\mathbf{f}(\mathbf{x}) = \mathbf{h}(\mathbf{x})\boldsymbol{\beta} = \mathbf{h}(\mathbf{x})\left(\frac{\mathbf{I}}{C} + \mathbf{H}^{\mathrm{T}}\mathbf{H}\right)^{-1}\mathbf{H}^{\mathrm{T}}\mathbf{T} \tag{6}$$

Finally, a given test sample belongs to the pattern corresponding to the output neuron with the maximum value.

Fusion method

New application of pattern recognition tools

As mentioned, the test samples were classified by ELM based on the principle of maximum value: the higher the value of an output-layer neuron, the higher the similarity of the sample to the corresponding pattern of this neuron, and *vice versa*. However, if a sample was simultaneously adjacent to the regions corresponding to multiple patterns in the vector space, or if the regions of such patterns were overlapping, this sample was considered highly similar to all these patterns. Therefore, the actual pattern of this sample might not correspond to the output-layer neuron with the maximum value.

The aforementioned case still held true in the pattern recognition of gas turbine performance degradation. As fig. 2 shows, where two falsely recognized degradation characteristic samples were taken, the value of each output-layer neuron was provided by ELM. Furthermore, considering that such false recognition results were not exclusive to ELM, the results given by the BPNN are also displayed in the figure.

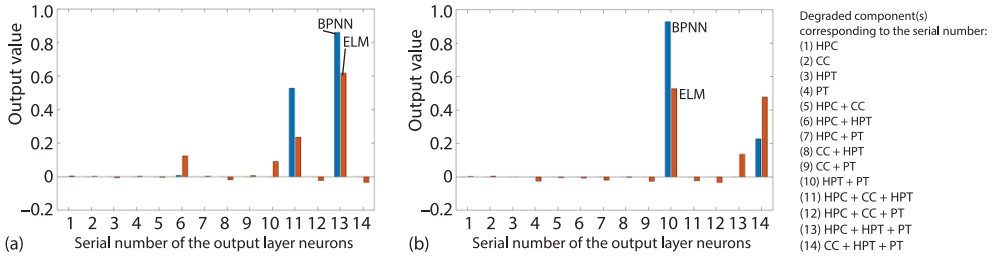

Figure 2. Values of output-layer neurons in BPNN and ELM for the same characteristic samples

As fig. 2(a) shows, among the recognition results provided by ELM, the degradation characteristic sample was highly similar to the 13th, 11th, 6th, and 10th degradation patterns. Regarding the recognition results of BPNN, the sample was of high similarity to the 13th and 11th degradation patterns. This sample belonged to the 11th degradation pattern, which, however, the two recognition tools mistakenly classified as the 13th pattern based on the principle of maximum value. Similarly, both ELM and BPNN mistakenly classified the 14th pattern as the 11th pattern, as fig. 2(b) shows.

Although both recognition tools provided incorrect results, the degradation characteristic sample showed high similarity to the actual degradation pattern, indicating that ELM and BPNN can be used as similarity ranking tools. Furthermore, ELM is a more appropriate alternative because it is of extremely fast learning speed and its output result more comprehensively embodies the similarity between the degradation characteristic sample and multiple degradation patterns.

Diagnosis process

The gas path diagnosis based on the fusion method took advantage of the fast similarity ranking of ELM and the accurate quantitative diagnosis of performance analysis models. By combining fig. 3, the complete diagnosis process could be divided into three-stages:

Train ELM. In this stage, the simulation model was used to generate the gas path measurable parameters of a gas turbine in a healthy status and those under multiple typical degradation patterns. On this basis, the degradation characteristic samples were extracted through eq. (7). Next, these samples and their patterns were utilized to construct a sample library and train ELM:

$$\overline{\mathrm{DC}} = \frac{\overline{\mathrm{MP}}_{\mathrm{Deg}} - \overline{\mathrm{MP}}_{\mathrm{Healthy}}}{\overline{\mathrm{MP}}_{\mathrm{Healthy}}} \tag{7}$$

where $\overline{\mathrm{MP}}_{\mathrm{Healthy}}$ and $\overline{\mathrm{MP}}_{\mathrm{Deg}}$ represent the gas path measurable parameters when the gas turbine was in the healthy status and a degradation status, respectively, DC is the degradation characteristic sample.

Extract the degradation characteristic sample of the practical gas turbine. In this stage, the actual operating data of the gas turbine to be diagnosed were collected, from which the extracted atmospheric parameters and operating condition parameters were input into the simulation model. After the gas path measurable parameters under the healthy status were acquired through simulation, the practical degradation characteristic sample could be similarly obtained using eq. (7).

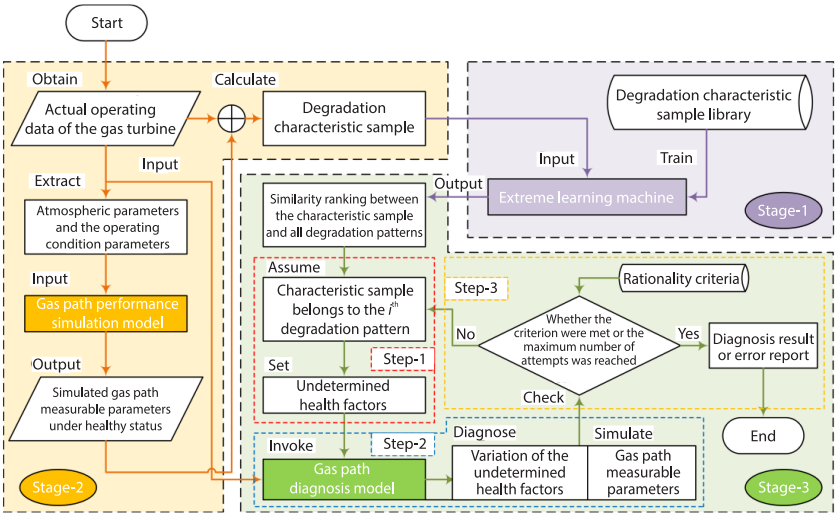

Figure 3. Flowchart of fusion method

Perform a quantitative diagnosis and verify the rationality of the results. As a core stage of the fusion method, this stage can be subdivided into three steps. Step-1 was pattern similarity ranking: the degradation characteristic sample was input into the trained ELM to acquire the similarity ranking among all degradation patterns. Step-2 was gas path diagnosis: the health factors corresponding to the degradation pattern with the highest similarity were set as the undetermined health factors, followed by a quantitative calculation using the diagnosis model. Step-3 was a rationality check: If the diagnosis result met all the rationality criteria, the calculated value of the undetermined health factors was accepted and output, and the diagnosis process was ended. Otherwise, the corresponding undetermined health factors would be calculated under the other high similarity degradation patterns according to the similarity ranking provided in Step-1 until a result meeting all the rationality criteria was acquired, or the maximum number of attempts was reached.

Two rationality criteria were proposed for the fusion method. First, the root mean square error between the simulated values (provided by the diagnosis model) and the measured values should be lower than the error threshold δ_{Error}. Second, the variation characteristic of the undetermined health factors should accord with that of the health factors under typical fault patterns [1, 2], as seen in tab. 1.

Table 1. Variation characteristics of health factors under typical fault patterns

Component	Fault pattern	Fault code	Variation characteristic	
			CMF	IE/CE
Compressor	Fouling	F1	<1	<1
	Erosion	F2	≈1	<1
	Tip clearance	F3	<1	≈1
	Foreign object damage	F4	≈1	<1
Combustion chamber	Carbon deposition	F5	≈1	<1
Turbine	Erosion	F6	>1	<1
	Fouling	F7	<1	<1
	Foreign object damage	F8	≈1	<1

Some undetermined health factors will be considered unchanged, that is, their variation characteristic belongs to ≈1 if their variation extent is lower than the healthy threshold δ_{Healthy}, which can avoid the adverse effect of measurement noise on the quantitative diagnosis and rationality check.

Application

The fusion method was applied to a GE LM2500+SAC gas turbine to verify its higher recognition rate and stronger robustness as well as its advantage in weakening the smearing effect. For comparison, the results acquired using three representative recognition tools – BPNN, SVM, and ELM – were also presented. In this section, the construction strategy of the degradation characteristic sample library, and the optimized hyper parameters in each recognition tool are provided.

Degradation characteristic sample library

The gas path structure and the sensor lay-out of GE LM2500+SAC gas turbine are shown in the *Appendix*, fig. A1. There were seven health factors, tab. 2, in total for this engine. However, the quantity of its measurable parameter used for gas path diagnosis was only six (except the atmospheric parameters, fuel temperature, and operating condition parameters). To obtain a unique solution to the diagnosis equations, it was assumed that the gas turbine only contained three components having performance degradation at most. Hence, there were four, six, and four single-, double-, and triple-component degradation patterns, respectively. After referring to the accepted empirical criteria [1, 2] and considering the common situations, the variation extent of each health factor under the aforementioned 14 degradation patterns was also provided in tab. 2.

Table 2. Variation of each health factor under different performance degradation patterns

Health factor	Variation extent		
	Single component	Double components	Triple components
$HF_{\text{HPC,CMF}}$	−0.01 ~ −0.07	−0.01 ~ −0.05	−0.01 ~ −0.03
$HF_{\text{HPC,IE}}$	−0.01 ~ −0.05	−0.01 ~ −0.04	−0.01 ~ −0.03
$HF_{\text{CC,CE}}$	−0.01 ~ −0.05	−0.01 ~ −0.04	−0.01 ~ −0.03
$HF_{\text{HPT,CMF}}$, $HF_{\text{PT,CMF}}$	−0.06 ~ +0.06	−0.04 ~ +0.04	−0.03 ~ +0.03
$HF_{\text{HPT,IE}}$, $HF_{\text{PT,IE}}$	−0.01 ~ −0.05	−0.01 ~ −0.03	−0.01 ~ −0.02

In addition, to ensure that simulation results approached the actual operating data, measurement noise was further added according to the accuracy of the gas path sensors. Unfortunately, the accuracy of each sensor cannot be disclosed due to it is the property of GE. In the follow-up generation of characteristic samples under each degradation pattern, the measurable parameters were denoised by 10-point averaging.

On this basis, a sample library can be constructed. Furthermore, the sample library was divided into three parts: a training set (Tr-1), a validation set (Va-1), and a test set (Te-1). In each set, the operating condition and degradation extent of the corresponding samples were uniformly distributed.

Hyper parameter setting

The hidden neuron number affected the recognition rate of BPNN and ELM. For ELM and SVM with kernel, their experiential risk and structural risk could be changed under the varying hyper parameters. Hence, these parameters should be optimized by focusing on the recognition rate of the validation set, which will allow for the best performance of recognition tools. Due to space constraints, the optimized results were given only. The neuron number was set as 20 and 600 for BPNN and ELM, respectively. Additionally, $C = 1024$ and $\sigma = 0.0156$ were set for ELM, and $C = 512$ and $\sigma = 2$ for SVM.

In the fusion method, the number of hidden-layer neurons, penalty factor C, and kernel parameter σ were identical to those in the case where it was used as the pattern recognition tool. During the quantitative diagnosis process (Stage-3), the maximum number of attempts was set as 3, and error threshold δ_{Error} and healthy threshold δ_{Healthy} were set as 0.005 and 0.003, respectively.

Results and analysis

Recognition effect

The different diagnosis methods were evaluated based on the test set Te-1. Table 3 lists the comparison results. The fusion method exhibited high capability with a false recognition rate of about 5.5%, 1.9%, and 0.64% under the single-, double- and triple-component degradation patterns, respectively.

Table 3. False recognition rates of BPNN, ELM, SVM, and fusion method

Degradation pattern	False recognition rate				False recognition type
	BPNN	ELM	SVM	Fusion method	
Single-component	19.6%	37.3%	13.1%	5.45%	Mostly belong to inclusion type
Double-component	8.03%	24.7%	7.51%	1.91%	
Triple-component	4.01%	4.09%	4.01%	0.64%	All belong to omission type
Total	8.17%	14.3%	7.08%	1.95%	

From tab. 3, the falsely recognized degradation patterns can be divided into two types: inclusion type or omission type. The former indicated that the recognized pattern not only contained all the components with actual performance degradation but also included those without performance degradation. Under this type, an accurate quantitative diagnosis result can be obtained if the diagnosis model was used. However, the latter was just the opposite and the acquired quantitative diagnosis result deviated significantly from the actual status of each component. A lower proportion of omission-type false recognitions manifested a higher accuracy of the quantitative result.

Robustness

The application effect of each diagnosis method was restricted by two factors:

– the simulation model generated the training samples, so they were not equivalent to the actual operating data of the gas turbine, making it difficult for the pattern recognition tool to be sufficiently trained and
– the hyper parameters influenced the recognition ability, but it took a long time to optimize them.

Whether the negative impact the aforementioned restrictions caused could be weakened was an important index to assess the robustness of the diagnosis method. In this section, the advantages of this fusion method are demonstrated in two cases.

In Case 1, the influence of the inequivalence between training samples and actual operating data on the recognition rate was explored. First, the measurement noise of six gas path measurable parameters was increased by 50% and embedded into the simulated results. Next, the various parameters were denoised by ten point averaging, thus building the Tr-2 and Te-2 with a higher noise level. Finally, Tr-1 and Tr-2 were used to train the BPNN, SVM, and ELM, and the recognition effect of each method was assessed using Te-1 and Te-2. The robustness of each was compared by taking the false recognition rate of the triple-component degradation patterns as an evaluation index, as fig. 4 shows.

As seen in fig. 4, when the same noise level was contained in both the training and test sets, the false recognition rates of the three tools were all about 4%. If a higher noise level was only added in the test set, their false recognition rates were elevated to about 5.5%. When a higher noise level was only added in the training set, their false recognition rates slightly declined to about 3.7%. The fusion method demonstrated the strongest robustness even under the harshest condition (Tr-1/Te-2), with a false recognition rate of only 1.5%. The comparison results revealed that the fusion method substantially weakens the negative influence of data inequivalence on the recognition effect.

In Case 2, the influence of improper hyper parameter settings on the recognition rate of each method was explored. First, the hyper parameters of ELM and SVM were set at some unreasonable values ($C = 2$, $\sigma = 0.5$). Then, each tool was trained using Tr-1 and assessed using Te-1, as fig. 5 shows.

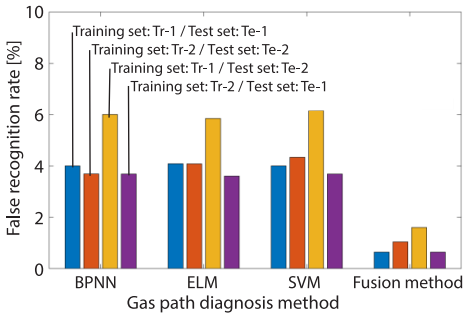

Figure 4. Noise influence on recognition effects of different methods

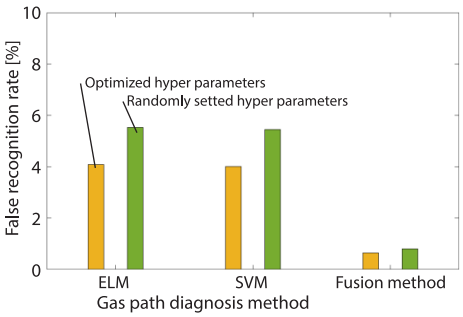

Figure 5. Influences of improper setting of hyper parameters on recognition effects of different methods

For ELM and SVM, the false recognition rate of the triple-component performance degradation patterns was increased from about 4-5.5% after the hyper parameters resetting. For the fusion method, however, the rate was just slightly elevated by about 0.16%. The results indicated that the recognition capability of this fusion method was insensitive to the value of hyper parameters.

Elimination of smearing effect

Benefiting from the higher recognition rate and stronger robustness, this fusion method had the advantage of eliminating the smearing effect.

In fig. 6, double- and triple-component degradation patterns were taken to display the variation of health factors in the following cases:

– embedded values,
– diagnostic values when the diagnosis equations were underdetermined,
– diagnostic values when the degradation pattern was falsely recognized, and
– diagnostic values based on the fusion method.

As fig. 6(a) depicts, if the diagnosis equations were underdetermined under a double-component degradation pattern (degraded components: CC and PT), all the components with degradation to a certain degree were considered. If a diagnosis was made under a falsely recognized degradation pattern (omission type), the decline of the CC combustion efficiency could not be found.

As fig. 6(b) shows, under a triple-component degradation pattern (degraded components: HPC, CC, and HPT), catastrophic impacts were brought to the quantitative diagnosis results if the diagnosis equations were underdetermined or if the degradation pattern was falsely recognized. To be specific, the decline of HPC flow capacity, the decrease of CC combustion efficiency, and the descent of HPT flow capacity were not effectively diagnosed. Furthermore, it was falsely considered that the PT flow capacity was increased. In striking contrast, the diagnosis results provided by the fusion method kept highly consistent with the actual situation.

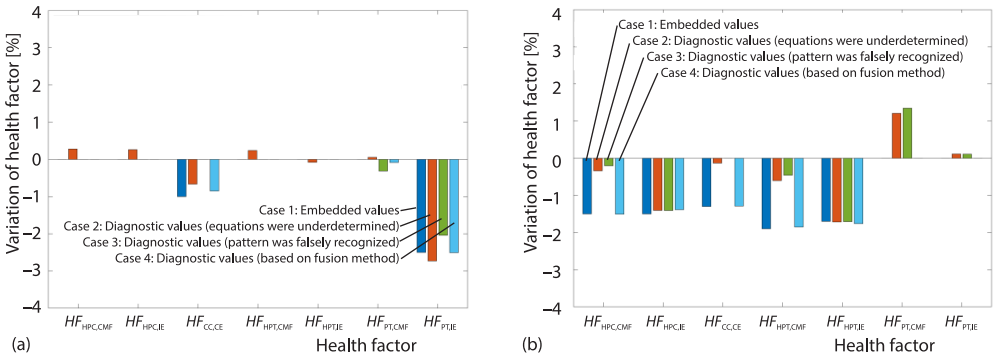

Figure 6. Diagnostic value of health factors based on different methods

Analysis

The fusion method constructs a new working mechanism of similarity ranking – gas path diagnosis – rationality check, which is a determinant of its higher recognition rate, stronger robustness, and higher diagnostic accuracy.

Specifically, the similarity ranking process narrows the search scope of degradation patterns. Therefore, the real-time feature of the complete process is ensured by reducing the number of tentative diagnoses. After each tentative diagnosis is completed, the assumed degradation pattern is determined by checking the convergence of iteration and the variation characteristic of the undetermined health factors. Hence, while improving the recognition rate, the fusion method also guarantees the accuracy of the follow-up quantitative diagnosis results.

To demonstrate the repeatability of the fusion method, data generated in the process of similarity ranking, gas path diagnosis, and rationality check of the cases shown in fig. 6 are listed in tabs. A1 and A2 in the *Appendix*. Furthermore, tab. A3 shows the environment parameters, fuel parameters, and engine health conditions of the two cases.

Conclusions

In this paper, a gas turbine diagnosis method fusing ELM and the performance analysis model was presented. In the fusion method, ELM aims to rank the similarity between the degradation characteristic sample and all the degradation patterns. In the performance analysis models, the diagnosis model is used to quantify the corresponding undetermined health factors under a minority of highly similar degradation patterns. The quantification result can be output only when rationality is satisfied. This method was verified with an GE LM2500+SAC gas turbine, and the following conclusions are as follows.

- Based on the working mechanism of similarity ranking – gas path diagnosis – rationality check, the fusion method can discover and correct the false result the pattern recognition tool provides.
- The fusion method can inhibit the negative impacts generated by the improper hyper parameters setting and the inequivalence between training samples and actual operating data on pattern recognition.
- Based on the higher recognition rate, the fusion method effectively eliminates the smearing effect, that is, the provided results can accurately reflect the health status of the actual gas turbine.

Nomenclature

C – penalty factor
HF – health factor

Greek letters

δ – threshold
σ – kernel parameter

Acronyms

ATM – atmosphere
C – combustion chamber
CE – combustion efficiency
CMF – corrected mass-flow
GG – gas generator
HPC – high pressure compressor
HPT – high pressure turbine
IE – isentropic efficiency
PT – power turbine

Appendix

Figure A1 shows the gas path structure and the lay-out of gas path sensors of GE LM2500+SAC. The six gas path measurable parameters used for diagnosis, were shown in red and bold text.

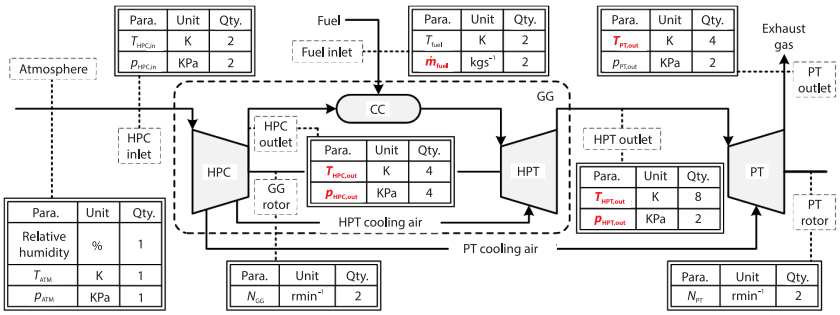

Figure A1. Gas path structure and the sensor lay-out of GE LM2500+SAC gas turbine (*for color image see journal web site*)

Corresponding to the diagnosis cases shown in fig. 6, tabs. A1 and A2 listed the data generated in Stage-3 (that is the step for similarity rank, gas path diagnosis, and rationality check) of this fusion method, respectively.

Table A1. Data generated in Stage-3 of this fusion method in the diagnosis case shown in fig. 6(a)

Diagnosis procedure	Procedure parameter	Gas path measurable parameters					
		$T_{HPC,Out}$	$p_{HPC,Out}$	$\dot{m}_{Fuel}$	$T_{HPT,Out}$	$p_{HPT,Out}$	$T_{PT,Out}$
Extract the degradation characteristic sample	$\overline{MP}_{Deg}$	711.8	1.876	1.204	1013	387.4	764.2
	$\overline{MP}_{Healthy}$	712.9	1.885	1.199	1014	388.4	756.8
	$\overline{DC}$	−0.1555%	−0.4678%	+0.4231%	−0.04262%	−0.2630%	+0.9693%
		Diagnosis result of health factors					
Similarity rank	Degradation pattern	1st: PT		2nd: CC + PT		3rd: HPC + CC + PT	
Gas path diagnosis	Undetermined health factors	$HF_{PT,CMF} \approx 1$ $HF_{PT,IE} = 0.9796$		$HF_{CC,CE} = 0.9915$ $HF_{PT,CMF} \approx 1$ $HF_{PT,IE} = 0.9749$		(Diagnosis is ended)	
Rationality check	Root mean square error	0.0067†	×	0.0019	√	–	–
	Fault code	F8	√	F5+F8	√	–	–

† The root mean square error exceeds the error threshold δ_{Error} ($\delta_{Error} = 0.005$).

Table A2. Data generated in Stage-3 of this fusion method in the diagnosis case shown in fig. 6(b)

Diagnosis procedure	Procedure parameter	Gas path measurable parameters					
		$T_{HPC,Out}$	$p_{HPC,Out}$	$\dot{m}_{Fuel}$	$T_{HPT,Out}$	$p_{HPT,Out}$	$T_{PT,Out}$
Extract the degradation characteristic sample	$\overline{MP}_{Deg}$	753.0	221.0	1.571	1126	0.4505	818.2
	$\overline{MP}_{Healthy}$	742.8	216.9	1.490	1088	0.4486	789.7
	$\overline{DC}$	+1.380%	+1.912%	+5.410%	+3.513%	+0.4284%	+3.611%
		Diagnosis result of health factors					
Similarity rank	Degradation pattern	1st: HPC + HPT + PT		2nd: HPC + CC + HPT		3rd : HPC + HPT	
Gas path diagnosis	Undetermined health factors	$HF_{HPC,CM}F \approx 1$ $HF_{HPC,IE} = 0.9859$ $HF_{HPT,CMF} = 0.9954$ $HF_{HPT,IE} = 0.9829$ $HF_{PT,CMF} = 1.0135$†† $HF_{PT,IE} \approx 1$††		$HF_{HPC,CMF} = 0.9849$ $HF_{HPC,IE} = 0.9861$ $HF_{CC,CE} = 0.9871$ $HF_{HPT,CMF} = 0.9815$ $HF_{HPT,IE} = 0.9824$		(Diagnosis is ended)	
Rationality check	Root mean square error	0.0013	√	0.0009	√	–	–
	Fault code	Error	×	F1 + F5 + F7	√	–	–

†† The variation characteristics of the two health factors do not agree with those of the health factors under typical fault patterns (shown in tab. 1).

Table A3 provides the environment parameters, fuel parameters, and engine health conditions corresponding to the diagnosis cases shown in figs. 6(a) and 6(b).

Table A3. The preset parameters in the diagnosis cases shown in figs. 6(a) and (b)

Case	Fuel parameters, environmental parameters, and operating condition parameters								
	Fuel parameters	Relative humidity	T_{ATM}	p_{ATM}	$T_{HPC,In}$	$p_{HPC,In}$	$p_{PT,Out}$	N_{GG}	N_{PT}
fig. 6(a)	Composition: CH4 (0.9506) C2H6 (0.0413) C3H8 (0.0081) Temperature: 328 K	60	288.3	101.1	288.3	101.0	101.3	9299	6100
		Engine health condition							
		$HF_{HPC,CMF} = 1$, $HF_{HPC,IE} = 1$, $HF_{CC,CE} = 0.99$ $HF_{HPT,CMF} = 1$, $HF_{HPT,IE} = 1$, $HF_{PT,CMF} = 1$, $HF_{PT,IE} = 0.975$							
fig. 6(b)		Relative humidity	T_{ATM}	p_{ATM}	$T_{HPC,In}$	$p_{HPC,In}$	$p_{PT,Out}$	N_{GG}	N_{PT}
		60	288.1	101.5	288.1	101.4	101.3	9501	6101
		Engine health condition							
		$HF_{HPC,CMF} = 0.985$, $HF_{HPC,IE} = 0.985$, $HF_{CC,CE} = 0.987$ $HF_{HPT,CMF} = 0.981$, $HF_{HPT,IE} = 0.983$, $HF_{PT,CMF} = 1$, $HF_{PT,IE} = 1$							

Reference

[1] Mohammadi, E., Montazeri-Gh, M., Simulation of Full and Part-Load Performance Deterioration of Industrial Two-Shaft Gas Turbine, *Journal of Engineering for Gas Turbines and Power*, *136* (2014), 9, pp. 092602-1-092602-9
[2] Yang, Q., *et al*, Full and Part-Load Performance Deterioration Analysis of Industrial Three-Shaft Gas Turbine Based on Genetic Algorithm, *Proceedings*, ASME Turbo Expo, Seoul, South Korea, 2016, Vol. 6, pp. V006T05A016
[3] Volponi, A. J., Gas Turbine Engine Health Management: Past, Present, and Future Trends, *Journal of Engineering for Gas Turbines and Power*, *136* (2014), 5, pp. 051201-1-051201-20
[4] Urban, L. A., Gas Path Analysis Applied to Turbine Engine Condition Monitoring, *Journal of Aircraft*, *10* (1973), 7, pp. 400-406
[5] Kamboukos, P., Mathioudakis, K., Comparison of Linear and Non-linear Gas Turbine Performance Diagnostics, Journal of Engineering for Gas Turbines and Power, 127 (2005), 1, pp. 49-56
[6] Stamatis, A., et al, Gas Turbine Component Fault Identification by Means of Adaptive Performance Modelling, *Proceedings*, ASME International Gas Turbine and Aeroengine Congress and Exposition, Brussels, Belgium, 1990, Vol. 5, pp. V005T15A015
[7] Li, Y. G., Non-Linear Weighted-Least-Squares Estimation Approach for Gas-Turbine Diagnostic Applications, *Journal of Propulsion and Power*, *27* (2011), 2, pp. 337-345
[8] Li, Y. G., Gas Turbine Performance and Health Status Estimation Using Adaptive Gas Path Analysis, *Journal of Engineering for Gas Turbines and Power*, *132* (2010), 4, pp. 041701-1-041701-9
[9] Stamatis, A., *et al*., Jet Engine Fault Detection with Discrete Operating Points Gas Path Analysis, *Journal of Propulsion and Power*, *7* (1991), 6, pp. 1043-1048
[10] Mathioudakis, K., *et al.*, Turbofan Performance Deterioration Tracking Using Non-Linear Models and Optimization Techniques, *Journal of Turbomachinery*, *124* (2002), 4, pp. 580-587
[11] Aretakis, N., *et al*., Non-Linear Engine Component Fault Diagnosis From a Limited Number of Measurements Using a Combinatorial Approach, *Journal of Engineering for Gas Turbines and Power*, *125* (2003), 3, pp. 642-650
[12] Mathioudakis, K., *et al.*, Gas Turbine Component Fault Detection from a Limited Number of Measurements, Proceedings of the Institution of Mechanical Engineers – Part A: *Journal of Power and Energy*, *218* (2004), 8, pp. 609-618
[13] Borguet, S., Leonard, O., Constrained Sparse Estimation for Improved Fault Isolation, *Journal of Engineering for Gas Turbines and Power*, *133* (2011), 12, pp. 121602-1-121602-8
[14] Torella, G., Lombardo, G., Neural Networks for the Diagnostics of Gas Turbine Engines, *Proceedings*, ASME Turbo Asia Conference, Jakarta, Indonesia, 1996, pp. V001T03A006

[15] Lu, P., *et al*., An Evaluation of Engine Faults Diagnostics Using Artificial Neural Networks, *Journal of Engineering for Gas Turbines and Power*, *123* (2001), 2, pp. 340-346
[16] Matuck, G. R., *et al*., Multiple Faults Detection of Gas Turbine by MLP Neural Network, *Proceedings*, ASME Turbo Expo, Power for Land, Sea, and Air, Orlando, USA, 2009, Vol.1, pp. 697-703
[17] Fast, M., *et al*., Development and Multi-Utility of an ANN Model for an Industrial Gas Turbine, *Applied Energy*, *86* (2009), 1, pp. 9-17
[18] Barad, S. G., *et al*., Neural Network Approach for a Combined Performance and Mechanical Health Monitoring of a Gas Turbine Engine, *Mechanical Systems and Signal Processing*, *27* (2012), Feb., pp. 729-742
[19] Zhou, D., *et al*., A New Gas Path Fault Diagnostic Method of Gas Turbine based on Support Vector Machine, *Journal of Engineering for Gas Turbines and Power*, *137* (2015), 10, pp. 102605-1-102605-6
[20] Huang, Q., *et al.*, A Kind of Approach for Aero Engine Gas Path Fault Diagnosis, *Proceeding*s, IEEE International Conference on Prognostics and Health Management, Dallas, Tex., USA, 2017, pp. 55-60
[21] Butler, S. W., *et al*., An Assessment Methodology for Data-Driven and Model-Based Techniques for Engine Health Monitoring, *Proceedings*, ASME Turbo Expo, Power for Land, Sea, and Air, Barcelona, Spain, 2006, pp. 823-831
[22] Lan, G., *et al*, Comparison and Fusion of Various Classification Methods Applied to Aero-Engine Fault Diagnosis, *Proceedings*, 29th Chinese Control and Decision Conference, Chongqing, China, 2017, pp. 4754-4759
[23] Huang, G. B., *et al*, Extreme Learning Machine: A New Learning Scheme of Feedforward Neural Networks, *Proceeding*s, IEEE International Joint Conference on Neural Networks, Budapest, Hungary, 2004, pp. 985-990
[24] Huang, G. B., *et al*., Extreme Learning Machine for Regression and Multiclass Classification, IEEE Transactions on Systems, *Man, and Cybernetics, Part B*, *42* (2012), 2, pp. 513-529
[25] Bartlett, P. L., The Sample Complexity of Pattern Classification with Neural Networks: The Size of the Weights is More Important than the Size of the Network, *IEEE Transactions on Information Theory*, *44* (1998), 2, pp. 525-536

Paper submitted: May 9, 2022
Paper revised: October 31, 2022
Paper accepted: November 1, 2022